*Supporting Information for*

# Vapor-Phase Pillarization of MXene for Engineering Hierarchical Interlayer Porosity

Song Luo[1,¶], Ali Kamali[1,¶], Joshua M. Little[2], Akash Warty[1], Jong K. Keum[3], Po-Yen Chen[2], Yeonsu Kwak[1], Hyunjik K. Kim[1], Dionisios G. Vlachos[1], Ke Zhang[4], John Yang[4], Dongxia Liu[1,*]

[1] Department of Chemical and Biomolecular Engineering, University of Delaware, Delaware, DE 19716, USA

[2] Department of Chemical and Biomolecular Engineering, University of Maryland, College Park, MD 20742, USA

[3] Center for Nanophase Materials Sciences and Neutron Scattering Division, Oak Ridge National Laboratory, Oak Ridge, TN 37830, USA

[4] Aramco Research Center – Houston, Saudi Aramco, Houston, TX 77077, USA

¶ These authors contributed equally: Song Luo, Ali Kamali

* Corresponding author:
Prof. Dongxia Liu
Email: liud@udel.edu
Phone: (+1) 302-831-6725

## S1. VPP of MXene without DDA or DDA separated from MXene

For comparison, two control experiments were conducted. One experiment was performed using a MXene/DDA ratio of 10, but with DDA placed outside the MXene compartment. The other experiment was carried out without usage of DDA in the intercalation stage. The isotherms of the resulting materials closely resembled that of pristine MXene (**Figure S1a**), indicating minimal interlayer expansion and limited TEOS access. The pore size distribtion data (**Figure S1b**) shows a minimal increase in pore sizes in both cases compared to those of MXene material.

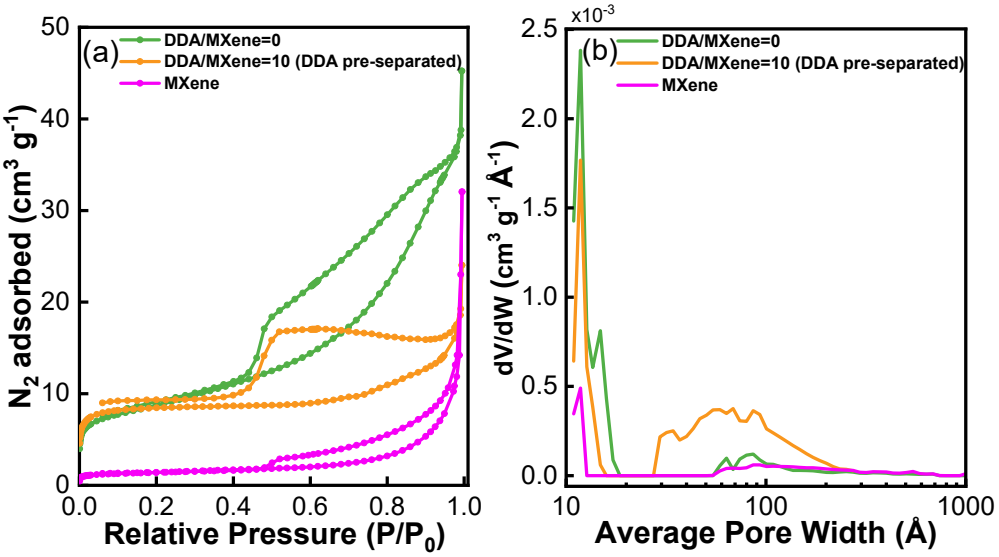


**Figure S1:** $N_2$ adsorption-desorption isotherms (a) and the corresponding pore size distributions (d) of P-MXene synthesized without DDA addition and with placement of both DDA and TEOS outside MXene container, respectivley. MXene sample is included for comparision. (P-MXene synthesis condition: MXene/DDA/TEOS/$H_2O$ = 1:10:0.5:10 (mass ratio), intercalation at 100 ℃, hydrolysis at 80 ℃)

## S2. Property of MAX material

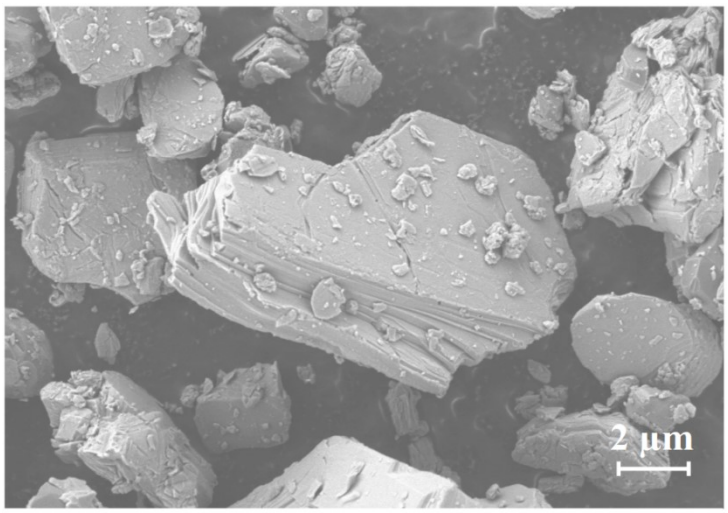


**Figure S2:** SEM image showing particle sizes and morphology of MAX phase.

## S3. Kinetics for DDA intercalation

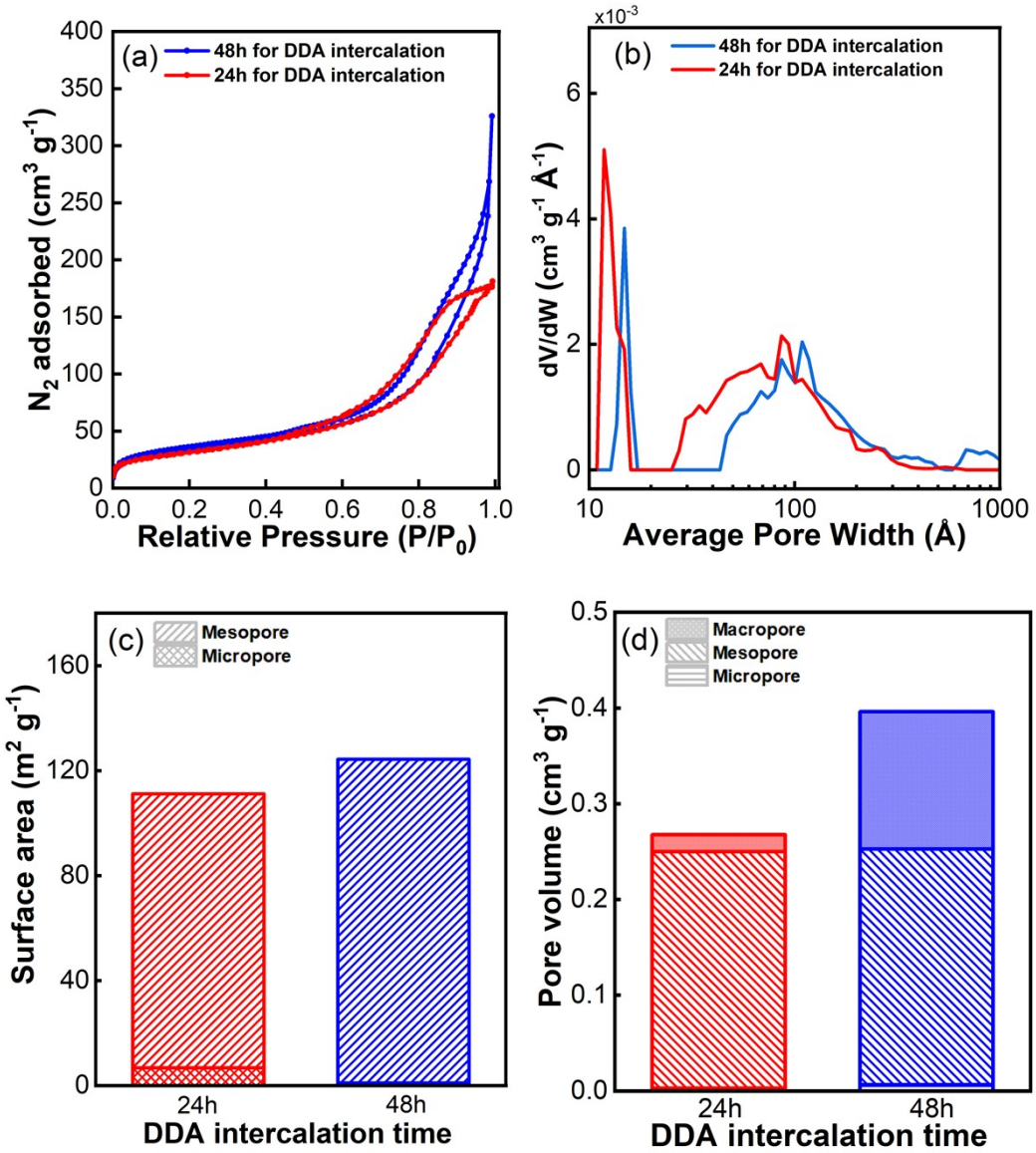


**Figure S3:** Textural properties of P-MXene synthesized using different DDA intercalation time. (a) $N_2$ adsorption-desorption isotherms; (b) pore-size distributions; (c) surface area partitioned into micro- and meso-contributions; (d) corresponding micro-, meso-, and macropore volumes. P-MXene synthesis condition: MXene/DDA/TEOS/$H_2O$ = 1:5:0.5:10 (mass ratio), intercalation at 100 ℃, hydrolysis at 80 ℃; the intercalation time was controlled at 24 and 48 h.

## S4. Thermogravity analysis (TGA) of MXene material

The TGA experiment was carried out on a thermo-gravimetric analyzer (TGA) (Shimadzu, TGA-50), during which the temperature was increased to 350 ℃ under flowing air (0.833 mL/s, breathing grade, Airgas) with a ramping rate of 0.167 ℃/s. The mass loss (~2 wt.%) up to ~120 ℃ is attributed to the adsorbed water in the MXene material.

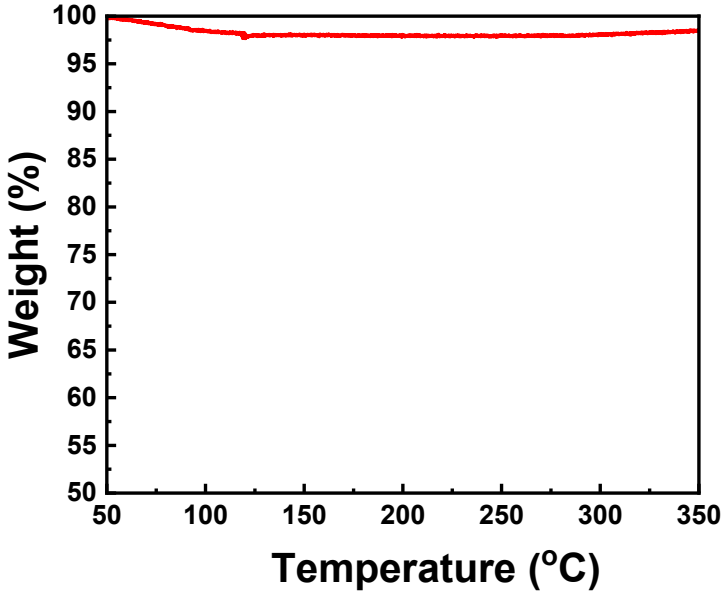


**Figure S4:** TGA result of the pristine MXene.

**S5. LDPE hydrogenolysis over Ru@P-MXene compared to P-MXene and Ru/C**

To evaluate the intrinsic contribution of the P-MXene support to the catalytic activity, LDPE hydrogenolysis was conducted over pristine P-MXene (without Ru loading) under the same reaction conditions as the Ru-loaded catalysts (LDPE-to-catalyst mass ratio of 20, 250 °C, 3.0 MPa $H_2$, 0.5 h). As shown in **Figure S5a**, the bare P-MXene support exhibited negligible LDPE conversion of only 2.8 %, with product yields of 0.1 % gas and 2.7 % liquid, while the vast majority of the feed remained as unconverted solid (97.2 %). In contrast, the 5.0 % Ru@P-MXene catalyst achieved 76.6 % LDPE conversion in just 30 min under identical temperature and pressure conditions, producing 56.4 % liquid and 15.5 % gas products with a solid residue of 23.4 %. The carbon balance closed at 100.0 % for the P-MXene control and 95.4 % for the 5.0 % Ru@P-MXene, with the minor deficit in the latter attributed to product losses during reactor-to-vial transfer and trace heavier products (> $C_{35}$) beyond the GC-FID calibration range. These results unequivocally confirm that the Ru metal species are the catalytically active sites responsible for LDPE hydrogenolysis, and that the P-MXene support alone does not enable appreciable C-C bond cleavage under the tested conditions.

The carbon number product distribution (**Figure S5b**) further illustrates the distinct roles of the support and the active metal. Over the pristine P-MXene, the trace products detected were distributed primarily in the $C_7$-$C_{15}$ (1.3 %) and $C_{16}$–$C_{26}$ (1.0 %) ranges, with no detectable methane formation (0 % $C_1$). The absence of methane and the predominance of heavier fragments suggest that the minimal conversion observed over bare P-MXene likely arises from non-catalytic thermal cracking of the LDPE at 250 °C, rather than from metal-catalyzed hydrogenolysis. In contrast, the 5.0 % Ru@P-MXene catalyst produced a broad product distribution spanning $C_1$ through $C_{35}$, with a methane yield of 12.3 % and the highest product yields concentrated in the $C_{16}$-$C_{26}$ range (27.0 %), followed by the $C_7$-$C_{15}$ range (18.1 %). The significant methane and light gas yields ($C_2$-$C_6$ = 5.7 %) observed exclusively in the Ru-loaded catalyst confirm that Ru facilitates both terminal and internal C-C bond scission pathways characteristic of metal-catalyzed hydrogenolysis, as discussed in our prior work.[32]

To benchmark the P-MXene support against a conventional catalyst support, we compared the catalytic performance of the commercial 5.0 % Ru/C catalyst with that of 5.0 % Ru@P-MXene under equivalent reaction conditions (LDPE-to-catalyst mass ratio of 20, 250 °C, 3.0 MPa $H_2$). As shown in **Figure S6a**, the 5.0 % Ru/C catalyst achieved 83.1 % LDPE conversion after 1 h, producing 51.3 % liquid and 31.1 % gas products with a solid residue of 16.9 %. In comparison, the 5.0 % Ru@P-MXene catalyst achieved a comparable conversion of 76.6 % in only 30 min, a reaction time two times shorter than that used for Ru/C. Despite the shorter reaction time, the liquid product yield over Ru@P-MXene (56.4 %) surpassed that of Ru/C (51.3 %), while the total gas yield was substantially lower (15.5 % compared to 31.1 %). The carbon balance closed at 99.3 % for Ru/C and 95.4 % for Ru@P-MXene. These results demonstrate that the P-MXene support not only enables a significantly faster reaction rate but also shifts the product distribution toward higher-value liquid products at the expense of less desirable gaseous products.

The carbon number distributions (**Figure S6b**) provide further insight into the selectivity differences between the two catalysts. The 5.0 % Ru/C catalyst exhibited a methane ($C_1$) yield of 25.1 %, approximately twice that observed over 5.0 % Ru@P-MXene (12.3 %). Beyond methane, the $C_2$-$C_6$ gas fraction was also higher over Ru/C (8.7 % compared to 5.7 %). Conversely, the Ru@P-MXene catalyst demonstrated superior selectivity toward the heavier liquid fractions, particularly in the $C_{16}$-$C_{26}$ range (27.0 % compared to 22.3 %). These observations are consistent with our prior findings,[32] in which Ru/C was shown to promote more extensive cascading C-C scission reactions that produce excess methane, while the confinement of Ru particles within the P-MXene interlayer spacing suppresses over-cracking by limiting polymer chain accessibility to the active sites and facilitating hydrogen availability through reverse spillover from the MXene substrate. The combined fuel-range liquid yield ($C_7$-$C_{26}$) was 45.1 % for the Ru@P-MXene catalyst compared to 43.4 % for Ru/C. Taken together, the substantially higher reaction rate, superior liquid selectivity, and suppressed methane formation over 5.0 % Ru@P-MXene underscore the advantage of the pillared MXene architecture as a catalyst support for polyolefin hydrogenolysis.

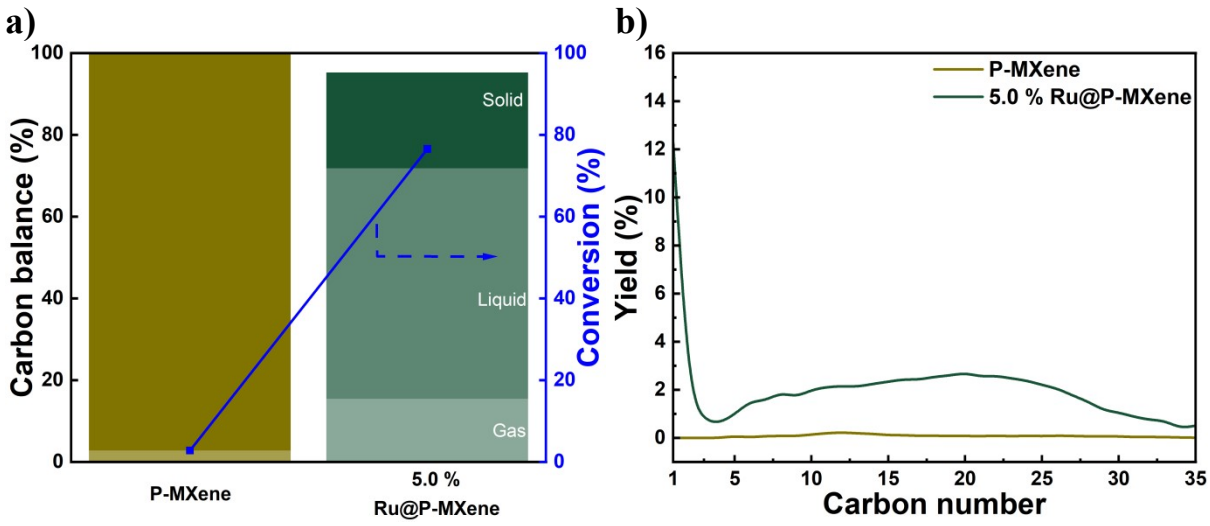


**Figure S5:** Conversion and product selectivity (a) and product yield distribution (b) from LDPE hydrogenolysis over P-MXene and Ru@P-MXene catalysts. Reaction conditions: 250 °C, 30 bar $H_2$, LDPE feed/catalyst mass ratio = 20. The reaction time was 0.5 h. (P-MXene synthesis condition: MXene/DDA/TEOS/$H_2O$ = 1:10:0.5:10 (mass ratio), intercalation at 100 °C, hydrolysis at 80 °C).

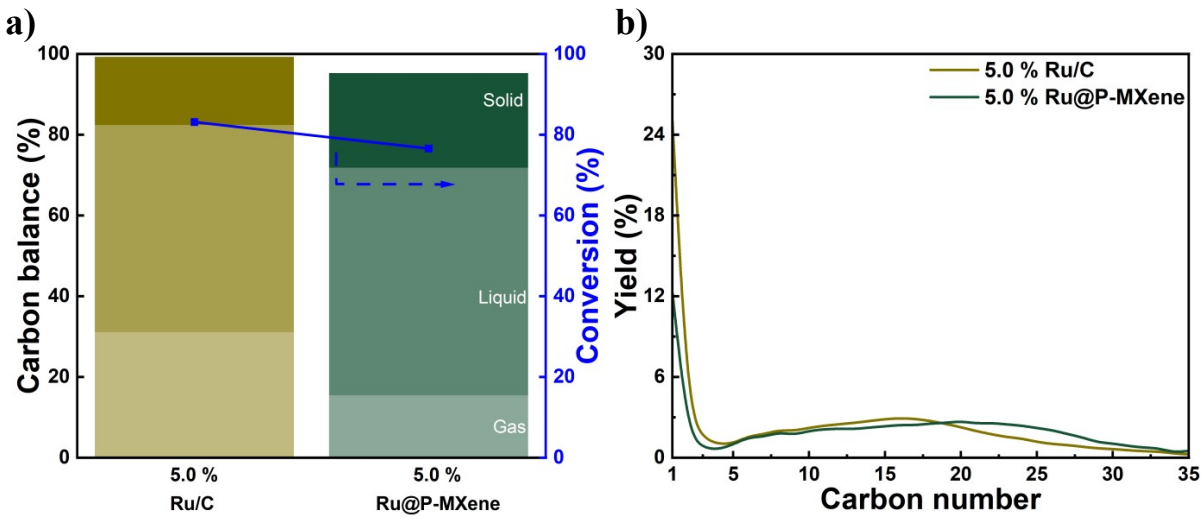


**Figure S6:** Conversion and product selectivity (a) and product yield distribution (b) from LDPE hydrogenolysis over Ru/C and Ru@P-MXene catalysts. Reaction conditions: 250 °C, 30 bar $H_2$, LDPE feed/catalyst mass ratio = 20. The reaction time for Ru/C and Ru@P-MXene was 1 and 0.5 h, respectively. (P-MXene synthesis condition: MXene/DDA/TEOS/$H_2O$ = 1:10:0.5:10 (mass ratio), intercalation at 100 °C, hydrolysis at 80 °C).

## S6. Textural properties of PMXene synthesized by VPP approach

**Table S1:** Surface areas and pore volumes of MXene and P-MXene materials.

| Samples | Surface area ($m^2/g$) | | | Pore volume ($cm^3/g$) | | | |
|---|---|---|---|---|---|---|---|
| | BET | Micropore | Mesopore | Cumulative | Micropore | Mesopore | Macropore |
| **MXene** | 4 | 2 | 2 | 0.01 | 0.00 | 0.01 | 0.001 |
| **P-MXene*** **(base condition)** | 148 | 41 | 107 | 0.53 | 0.02 | 0.51 | 0.13 |

** Synthesis condition: VPP, MXene/DDA/TEOS/$H_2O$ = 1:10:0.5:10 (mass ratio), intercalation at 100 ℃, hydrolysis at 80 ℃.*

**Table S2:** Surface areas and pore volumes of P-MXene materials synthesized with varying DDA.

| Samples* | Surface area ($m^2/g$) | | | Pore volume ($cm^3/g$) | | | |
|---|---|---|---|---|---|---|---|
| | BET | Micropore | Mesopore | Cumulative | Micropore | Mesopore | Macropore |
| **DDA/MXene=20** | 67 | 3 | 64 | 0.2 | 0.001 | 0.2 | 0.068 |
| **DDA/MXene=10** | 148 | 41 | 107 | 0.53 | 0.02 | 0.51 | 0.13 |
| **DDA/MXene=5** | 111 | 7 | 104 | 0.25 | 0.003 | 0.25 | 0.018 |
| **DDA/MXene=0** | 26 | 21 | 5 | 0.02 | 0.011 | 0.01 | 0.013 |

** Synthesis condition: VPP, MXene/DDA/TEOS/$H_2O$ = 1:x:0.5:10 (mass ratio), intercalation at 100 ℃, hydrolysis at 80 ℃.*

**Table S3:** Surface areas and pore volumes of P-MXene materials synthesized with varying TEOS.

| Samples* | Surface area ($m^2/g$) | | | Pore volume ($cm^3/g$) | | | |
|---|---|---|---|---|---|---|---|
| | BET | Micropore | Mesopore | Cumulative | Micropore | Mesopore | Macropore |
| **TEOS/MXene=20** | 33 | 27 | 6 | 0.13 | 0.014 | 0.12 | 0.15 |
| **TEOS/MXene=1** | 39 | 21 | 18 | 0.14 | 0.011 | 0.13 | 0.002 |
| **TEOS/MXene=0.5** | 148 | 41 | 107 | 0.53 | 0.02 | 0.51 | 0.13 |
| **TEOS/MXene=0.1** | 86 | 0 | 86 | 0.18 | 0 | 0.18 | 0 |

** Synthesis condition: VPP, MXene/DDA/TEOS/$H_2O$ = 1:10:x:10 (mass ratio), intercalation at 100 ℃, hydrolysis at 80 ℃.*

**Table S4:** Surface areas and pore volumes of P-MXene materials synthesized with varying water.

| Samples* | Surface area ($m^2/g$) | | | Pore volume ($cm^3/g$) | | | |
|---|---|---|---|---|---|---|---|
| | BET | Micropore | Mesopore | Cumulative | Micropore | Mesopore | Macropore |
| **Water/MXene=20** | 72 | 17 | 55 | 0.2 | 0.009 | 0.19 | 0.033 |
| **Water/MXene=10** | 148 | 41 | 107 | 0.53 | 0.02 | 0.51 | 0.13 |
| **Water/MXene=0** | 100 | 5 | 95 | 0.24 | 0.002 | 0.24 | 0.088 |

** Synthesis condition: VPP, MXene/DDA/TEOS/$H_2O$ = 1:10:0.5:x (mass ratio), intercalation at 100 ℃, hydrolysis at 80 ℃.*

**Table S5:** Surface areas and pore volumes of P-MXene materials synthesized with HA, DDA, or ODA.

| Samples* | Surface area ($m^2/g$) | | | Pore volume ($cm^3/g$) | | | |
|---|---|---|---|---|---|---|---|
| | BET | Micropore | Mesopore | Cumulative | Micropore | Mesopore | Macropore |
| **ODA** | 125 | 28 | 97 | 0.25 | 0.015 | 0.24 | 0.04 |
| **DDA** | 148 | 41 | 107 | 0.53 | 0.02 | 0.51 | 0.13 |
| **HA** | 100 | 16 | 84 | 0.29 | 0.008 | 0.28 | 0.1 |

** Synthesis condition: VPP, MXene/HA, DDA or ODA/TEOS/$H_2O$ = 1:10:0.5:10 (mass ratio), intercalation at 100 ℃, hydrolysis at 80 ℃.*

**Table S6:** Surface areas and pore volumes of P-MXene materials synthesized with varying TEOS.

| Samples* | Surface area ($m^2/g$) | | | Pore volume ($cm^3/g$) | | | |
|---|---|---|---|---|---|---|---|
| | BET | Micropore | Mesopore | Cumulative | Micropore | Mesopore | Macropore |
| **TEOS/MXene=20** | 390 | 14 | 376 | 0.43 | 0.005 | 0.43 | 0.024 |
| **TEOS/MXene=10** | 352 | 42 | 310 | 0.47 | 0.021 | 0.45 | 0.052 |
| **TEOS/MXene=6.4** | 386 | 92 | 294 | 0.27 | 0.046 | 0.22 | 0.082 |
| **TEOS/MXene=3.2** | 188 | 33 | 155 | 0.26 | 0.017 | 0.24 | 0.055 |
| **TEOS/MXene=1.6** | 180 | 7 | 173 | 0.42 | 0.003 | 0.42 | 0.2 |

** Synthesis condition: VPP, MXene/DDA/TEOS/$H_2O$ = 1:0.8:x:10 (mass ratio), intercalation at 100 ℃, hydrolysis at 80 ℃.*

**Table S7:** Surface areas and pore volumes of P-MXene materials synthesized with varying intercalation temperature.

| Samples* | Surface area ($m^2/g$) | | | Pore volume ($cm^3/g$) | | | |
|---|---|---|---|---|---|---|---|
| | BET | Micropore | Mesopore | Cumulative | Micropore | Mesopore | Macropore |
| **170 ℃** | 257 | 87 | 170 | 0.23 | 0.045 | 0.18 | 0.008 |
| **130 ℃** | 310 | 49 | 261 | 0.45 | 0.025 | 0.43 | 0.099 |
| **100 ℃** | 386 | 92 | 294 | 0.27 | 0.046 | 0.22 | 0.082 |
| **80 ℃** | 309 | 20 | 289 | 0.43 | 0.009 | 0.42 | 0.067 |

** Synthesis condition: VPP, MXene/DDA/TEOS/$H_2O$ = 1:0.8:6.4:10 (mass ratio), intercalation at 80, 100, 130, or 170 ℃, hydrolysis at 80 ℃.*

## S7. Detailed experimental and analytical procedures for LDPE hydrogenolysis

Following the procedure established in our prior work,[1] the reaction products were collected after quenching the reactor in an ice bath once the temperature dropped below 3.0 °C. The product stream was separated into three phases: gas, liquid, and solid. The gaseous products ($C_{1–4}$) were extracted from the reactor headspace into a 1.0 L Tedlar gas sampling bag and analyzed by gas chromatography with a flame-ionization detector (GC-FID, Agilent) equipped with a CP-Volamine GC column. The residual solid and oil/liquid mixture remaining inside the reactor were dissolved in approximately 20 mL of methylene chloride ($CH_2Cl_2$) containing 20 mg of n-octacosane ($C_{28}H_{58}$) as an external standard. The resulting slurry was filtered through Whatman filter paper (GE, 11 μm) to separate the soluble fraction, categorized as liquid products ($C_{5–35}$), from the insoluble solid residue retained on the filter paper. The liquid products were quantified using a GC-FID (Agilent) equipped with an HP-1 column and identified by gas chromatography coupled with mass spectrometry (GC-MS, Agilent) equipped with a DB-1 column. Analytical standard calibration mixtures spanning $C_1$ to $C_{35}$ were employed to determine calibration coefficients (i.e., response factors) and retention times for product identification. The n-octacosane external standard enabled the absolute quantification of each liquid product by relating the GC-FID peak areas to known mass concentrations. The products primarily consisted of linear alkanes with a minor fraction of branched alkanes; no aromatics were identified in any of the experiments.

The yields of liquid and gas products were calculated on a carbon molar basis following the methodology described in our previous publication.[1] The yield of the product group with i carbons ($Y_i$) was defined as $Y_i = n_i / n_{feed}$, where $n_i$ is the moles of carbon in the product group with i carbons and $n_{feed}$ is the total moles of carbon in the plastic feed. The overall LDPE conversion (X, %) was determined gravimetrically as $X = (m_{feed} - m_{residue}) / m_{feed} \times 100$, where $m_{feed}$ is the initial mass of the LDPE feed and $m_{residue}$ is the mass of the unconverted polymer residue collected on the filter paper. The solid yield ($Y_s$) was calculated as $Y_s = 100 – X(\%)$. The total gas yield was obtained by summing the individual $C_1$ through $C_4$ yields, while the total liquid yield was obtained by summing the $C_5$ through $C_{35}$ yields. The carbon balance was assessed to verify the accuracy and consistency of the product quantification. The overall carbon balance was computed as the sum of the solid, liquid, and gas yields (i.e., carbon balance = $Y_s + \Sigma Y_{liquid} + \Sigma Y_{gas}$), where the solid yield accounts for the unconverted polymer fraction determined gravimetrically, and the liquid and gas yields

account for all carbon-containing products quantified by GC-FID. Each experiment was evaluated for carbon balance closure, with acceptable values falling within the range of 90-100 %. Deviations from complete closure are attributed to minor product losses during the transfer of reactor contents to the methylene chloride solution, trace amounts of heavier products (> $C_{35}$) not captured by the GC-FID calibration range, and residual hydrocarbons adsorbed on the catalyst surface or reactor walls.

References

(1) Kamali, A.; Little, J. M.; Luo, S.; Chen, A.; Warty, A.; Bhowmick, A.; Moncada, J.; Jahrman, E. P.; Vance, B. C.; Keum, J. K.; Woehl, T. J.; Chen, P.-Y.; Vlachos, D. G.; Liu, D. Plastic-Waste Hydrogenolysis over Two-Dimensional MXene-Supported Ruthenium Catalysts with Tunable Interlayer Spacing. *Chem Catal.*